


Specific features of the conductivity and spin susceptibility tensors of a two-dimensional electron gas with Rashba and Dresselhaus spin-orbit interactions

Yu. Ya. Tkach ^{*}

Kotel'nikov Institute of Radio Engineering and Electronics, Russian Academy of Sciences, Moscow District, Fryazino 141190, Russia



(Received 7 April 2021; revised 17 June 2021; accepted 29 July 2021; published 11 August 2021; corrected 24 August 2021)

The two-dimensional electron gas with spin-orbit interactions (SOIs) of Rashba and Dresselhaus types is known to form an anisotropic system with a Van Hove singularity in the density of states. Moreover, the “amplitude” and the energy position of this singularity depend on the ratio of the constants of Rashba α and Dresselhaus β SOIs, $\gamma = \beta/\alpha$. Here the dependencies of the conductivity and spin susceptibility tensors on the position of the Fermi level are calculated for a wide range of γ . It is shown that if only the lower spin subband is filled the diagonal elements of the conductivity tensor have dips that appear when the Fermi level passes the singularity point both for $\gamma < 1$ and $\gamma > 1$. The amplitude of these features and their energy position depend on γ and, in particular, for the state of persistent spin helix $\gamma = 1$ they disappear. When only the lower spin subband is filled, the off-diagonal elements of the conductivity tensor are nonzero, that is, there is a Hall voltage due to the anisotropy of the Fermi surface and the scattering. In the region of filling of two spin subbands the ratio of diagonal and nondiagonal components of the spin susceptibility tensor is equal to γ and in the conductivity tensor, the off-diagonal terms vanish.

DOI: [10.1103/PhysRevB.104.085413](https://doi.org/10.1103/PhysRevB.104.085413)

I. INTRODUCTION

Two-dimensional electron gas (2DEG) with spin-orbit interaction (SOI) has been the object of intensive research, both experimental [1–8] and theoretical [9–19], for many years. Although the energy spectrum of a 2DEG with a SOI has been well studied [19], recently it was shown [20] that the joint SOIs of Rashba and Dresselhaus lead to the appearance of a saddle point in the spectrum and to the logarithmic Van Hove singularity (VHS) in the density of states [21]. The energy position of the singularity depends on the ratio of the SOI constants γ . The energy spectrum in this setting was studied in more detail in Ref. [22]. It is easy to verify that with the standard dispersion law near the saddle point $E \approx E_s + c_x k_x^2 - c_y k_y^2$, the density of states has the form

$$N_s(E) \approx N_{so}(\gamma) - \frac{1}{\sqrt{c_x c_y}} \ln |E - E_s|. \quad (1)$$

Here N_{so} is a smooth part of density of states. For simplicity, we use dimensionless units which are explained below in the framework of the considered model. An important point is a factor in logarithmic VHS, which is determined by the curvatures of the saddle point. The singularity of the density of states manifests in transport phenomena when the following inequality is fulfilled:

$$N_{so} \ll \frac{1}{\sqrt{c_x c_y}}. \quad (2)$$

Otherwise the singularity becomes undetectable both in the density of states and in transport phenomena.

In recent works [23,24], the conductivity and spin susceptibility in the Aronov-Lyande-Geller-Edelstein (ALGE) effect [25,26] as a function of the position of the Fermi level have been studied in detail for the 2DEG system with the Rashba SOI. It was shown that in the case of low electron concentrations, when only one spin subband is filled, these dependencies have an unusual form. The conductivity is proportional to $E_F/E_{so} + (E_F/E_{so})^2$, and the spin susceptibility is proportional to E_F/E_{so} , where E_F is the Fermi energy and $E_{so} = m\alpha^2/(2\hbar^2)$ is the characteristic energy of the Rashba SOI (m is the effective electron mass). These dependencies calculated at low temperatures with allowance for the second spin subband for scattering by a short-range impurity potential are shown Fig. 1. The conductivity tensor G_{ij} was calculated using both the kinetic Boltzmann equation and quantum analysis based on the Kubo formula. The main result is an unconventional dc conductivity, when only the lower spin subband is filled and the Drude conductivity when the second spin subband is filled [23]. The ALGE effect was considered using the semiclassical Boltzmann transport theory [24].

In structures with Rashba SOI a volume symmetry is usually broken, that is, there is also the Dresselhaus SOI [1–5]. Hence a saddle point and a Van Hove singularity appear in the energy spectrum and the density of states, respectively [20]. This leads to a significant change in their transport properties. This work is devoted to study the dependencies of the conductivity and spin susceptibility tensors of the ALGE effect on the position of the Fermi level in a 2DEG with Rashba and Dresselhaus SOIs for the case of scattering by impurities with a short-range potential at low temperatures. The calculations are based on the method developed in Ref. [27]. It was shown that the kinetic Boltzmann equation in this formulation is the Fredholm equation with a degenerate kernel which can be

^{*}utkach@gmail.com

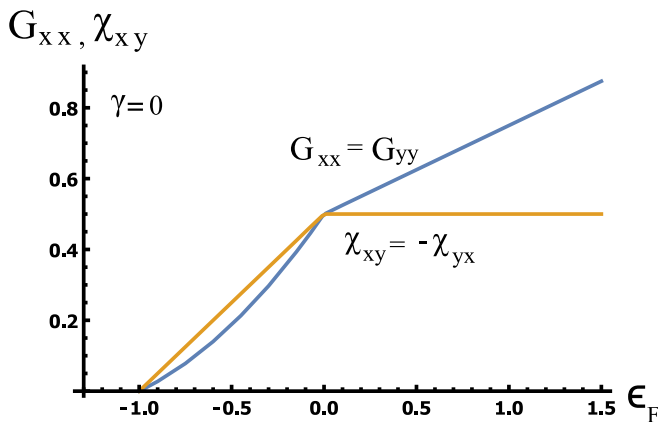


FIG. 1. Dependencies of the conductivity G_{ij} and spin susceptibility χ_{ij} tensor components on the position of the Fermi level for 2DEG with Rashba SOI. The energy here and below is normalized to E_{so} , and the normalization of conductivity and susceptibility are given below (see Figs. 4 and 5). $G_{xy} = G_{yx} = 0$ and $\chi_{xx} = \chi_{yy} = 0$.

easily reduced to a linear equation and solved exactly. As a test of the efficiency of the developed method, we reproduced the results of the papers [23,24] for the conductivity and spin susceptibility of 2DEG with the Rashba SOI (see Fig. 1). In this work, we calculate the conductivity tensor and the spin susceptibility of the ALGE effect as a function of the position of the Fermi level for 2DEG with Rashba and Dresselhaus SOIs for a wide range of γ .

We list the main results obtained in the work. In the literature, there were no convincing calculations of the conductivity and spin susceptibility tensors for 2DEG with the Rashba and Dresselhaus spin-orbit interaction, especially for a low 2DEG concentration, when only the lower spin subband is filled. The method developed in a paper [27], allowed us to calculate these tensors with the required accuracy. As a result, we managed to find out that the Hall voltage can exist without a magnetic field. Note that recently an anomalous Hall voltage, that is, a voltage without a magnetic field, was observed in a twisted bilayer graphene [28]. In addition, it is surprising that the ratio of the SOI constants can be determined from the ratio of spin susceptibilities. In the state of a persistent spin helix there is no Van Hove singularity.

II. HAMILTONIAN AND ELECTRONIC STATES

We consider a two-dimensional electron gas without inversion symmetry, allowing SOI that is linear in the electron wave vector. The most general form of linear coupling includes both Rashba and Dresselhaus contributions and has the following form [29,30]:

$$H = \frac{\mathbf{p}^2}{2m}\sigma_0 + \frac{\alpha}{\hbar}(p_x\sigma_y - p_y\sigma_x) + \frac{\beta}{\hbar}(p_x\sigma_x - p_y\sigma_y). \quad (3)$$

Here $\mathbf{p} = (p_x, p_y)$ is the electron momentum, p_x and p_y being its components along the [100] and [010] directions of a zinc-blende crystal, respectively, and σ_x and σ_y are Pauli matrices. There are two types of eigenstates, which we will denote by the index $\lambda = \pm$. Their energies and wave functions

are of the form

$$\varepsilon_\lambda(\mathbf{k}) = k^2 + 2\lambda g(\mathbf{k}, \gamma) \quad (4)$$

and

$$\psi_{\mathbf{k}\lambda}(\mathbf{r}) = \frac{1}{\sqrt{2S^*}} \begin{pmatrix} 1 \\ i\lambda e^{i\varphi} \end{pmatrix} e^{i(k_x x + k_y y)}. \quad (5)$$

Here and below, we used dimensionless quantities: ε is energy normalized to the characteristic energy of the Rashba SOI E_{so} ; \mathbf{k} is a wave vector normalized to $k_{so} = \alpha m/\hbar^2$; $g(\mathbf{k}, \gamma) = \sqrt{(k_x - \gamma k_y)^2 + (k_y - \gamma k_x)^2}$, S^* is a sample area.

The phase $\varphi(\mathbf{k})$ is determined by the following relations:

$$\sin \varphi = \frac{(k_y - \gamma k_x)}{g(\mathbf{k}, \gamma)}, \quad (6)$$

$$\cos \varphi = \frac{(k_x - \gamma k_y)}{g(\mathbf{k}, \gamma)}. \quad (7)$$

A change in the SOI constants ratio leads to a great variety of Fermi contours and their significant rearrangement. A typical energy landscape corresponding to the dispersion law (4) is shown in Fig. 2 for two values of γ . According to expression (4), the energy landscape in the \mathbf{k} space is centrosymmetric $\varepsilon_\lambda(\mathbf{k}) = \varepsilon_\lambda(-\mathbf{k})$. Fermi contours have mirror symmetry along two axes $k_x = \pm k_y$. In the lower spin subband, there are two minima with the same energy $\varepsilon_{-,m} = -(1 + \gamma)^2$, spaced apart in \mathbf{k} space and having coordinates $\pm[(1 + \gamma)/\sqrt{2}, (1 + \gamma)/\sqrt{2}]$, as well as two saddle points with energy $\varepsilon_{-,s} = -(1 - \gamma)^2$ and coordinates $[\pm(1 - \gamma)/\sqrt{2}, \mp(1 - \gamma)/\sqrt{2}]$. Reducing the potential to canonical form near saddle points gives us the following expression for the dispersion law:

$$\varepsilon_{s,1,2} = -(1 - \gamma)^2 + 2q_x^2 - \frac{4\gamma(q_y \pm 1)^2}{(1 - \gamma)^2}, \quad (8)$$

where $q_x = (k_x + k_y)/\sqrt{2}$ and $q_y = (k_x - k_y)/\sqrt{2}$. This means that the density of states near the saddle points is given by relation (1), with the smooth part and the factor in the logarithmic term depending on γ :

$$N_s(E) \approx N_{so}(\gamma) - \frac{|1 - \gamma|}{\sqrt{2\gamma}} \ln |\varepsilon - \varepsilon_s|. \quad (9)$$

This result demonstrates that there are two singularities in the density of states with coinciding energies and shows the change in the amplitude of the singularity as a function of the SOI constants ratio γ . In particular, from (9) one can see that there is no Van Hove singularity in the state of persistent spin helix ($\gamma = 1$). These results are confirmed by numerical calculations of the density of states $N_s(\varepsilon)$ (see Fig. 3). To calculate the density of states numerically, the following relation is used:

$$N_s(\varepsilon) = \frac{1}{\pi^2} \lim_{\Delta\varepsilon \rightarrow 0} \sum_\lambda \frac{S_\lambda(\varepsilon + \Delta\varepsilon) - S_\lambda(\varepsilon)}{\Delta\varepsilon}. \quad (10)$$

Here $S_\lambda(\varepsilon)$ is the area of the region in the \mathbf{k} space, satisfying the inequality $\varepsilon_\lambda(\mathbf{k}) \leq \varepsilon$.

The Dirac point (point of tangency of two spin subbands) for $\gamma \neq 1$ is located at energy $\varepsilon_D = 0$ at a point with coordinates $(k_x = 0, k_y = 0)$ in \mathbf{k} space. For $\gamma = 1$, the Dirac point is transformed into a line $k_x = k_y$ (see Fig. 2).

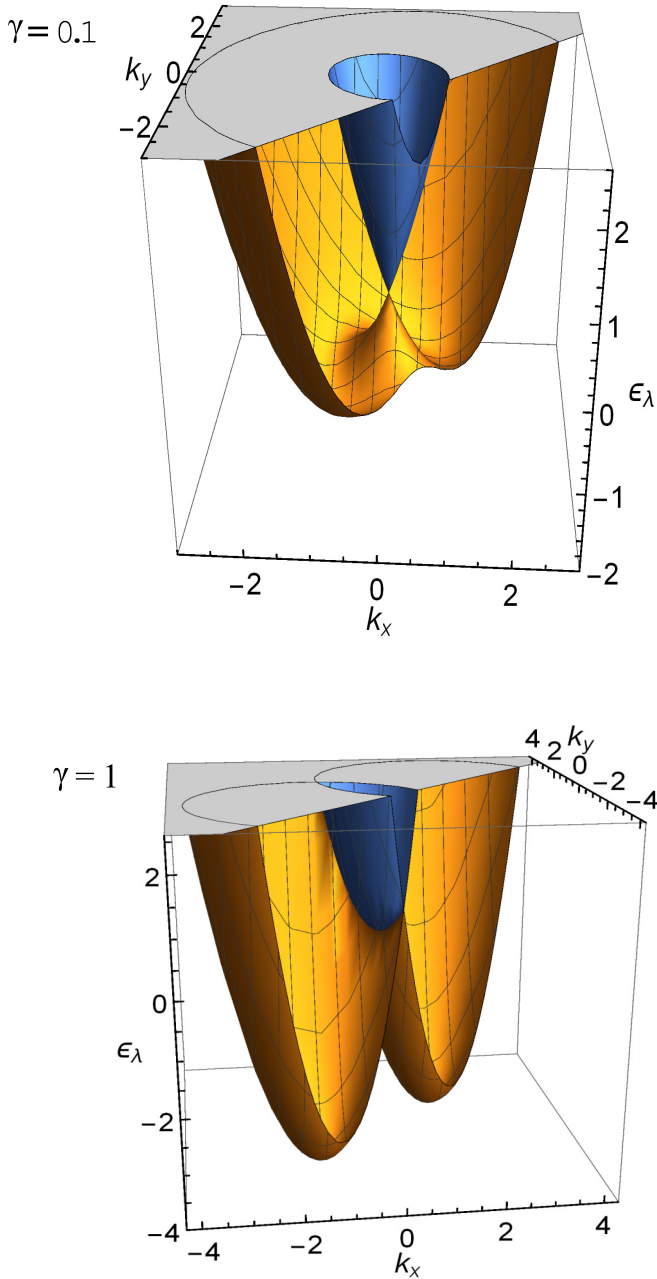


FIG. 2. A section of the energy landscape defined by Eq. (4) in the \mathbf{k} space. The blue and yellow surfaces correspond to $\lambda = +$ and $\lambda = -$, respectively, and their intersection is a Dirac point. Ratio of SOI constants $\gamma = 0.1$ and $\gamma = 1$.

Numerical calculations of the one-particle density of states also show that there is a density jump corresponding to the minimum of the dispersion law and a VHS corresponding to the saddle point, and the amplitude of this singularity is given by the relation $|1 - \gamma|/\sqrt{2\gamma}$. This, in particular, indicates that the VHS disappears at $\gamma = 1$ and reappears at $\gamma > 1$ with an amplitude increasing with the SOI constants ratio γ . Despite the wide variety of Fermi contours and their variation depending on the ratio of the SOI constants [20,22,27], the filling of the second spin subband makes the single-particle density of states independent of energy and equal to $N_o = m/(\pi\hbar^2)$.

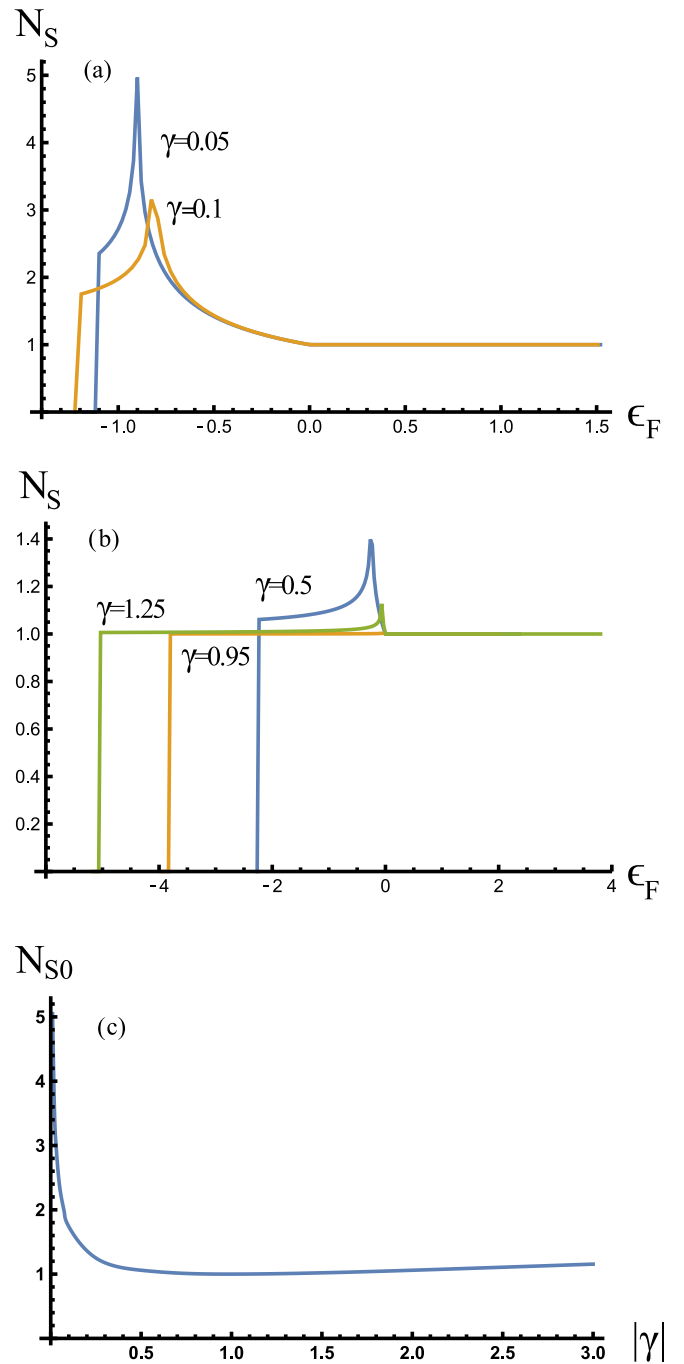


FIG. 3. Typical energy dependencies of the density of states for a wide range of SOI constant ratios γ (a),(b). N_S is normalized to $N_o = m/(\pi\hbar^2)$. The dependence of N_{so} from formula (1) on γ is shown in (c).

This is clearly seen from the calculations shown in Fig. 3 and from earlier calculations [20]. Thus, although the anisotropy of the Fermi contours is preserved, their multicomponent nature leads to this result. In this sense, we can talk about the conditional disappearance of an anisotropy in the system when filling above the Dirac point.

When calculating the density of states, we use the exact dispersion law, so the value of N_{so} in formula (1), of course, has a conditional meaning. In particular, its value may depend

on the direction of the energy change, as in our case. To the right of the VHS value N_{s_0} is approximately equal to 1, and to the left N_{s_0} is determined by the graph in Fig. 3(c) and equals the jump $N_s(\varepsilon)$ at the beginning of the spectrum.

III. BOLTZMANN KINETIC EQUATION AND ITS SOLUTION

Electron transport is studied using the semiclassical approach. For a small uniform electric field \mathcal{E} , the distribution function $f(\mathbf{k})$ is determined by the Boltzmann equation. The anisotropy of the dispersion law leads to the scattering anisotropy; therefore, the collision integral cannot be simplified by introducing the relaxation time. This problem has been discussed in detail in the literature [9,12–14].

We consider scattering by impurities with a short-range potential $V(r) = V_0\delta(\mathbf{r})$. The impurity concentration N is assumed to be sufficiently low so that the scattering by different impurities is not correlated. Using the wave functions (5) and calculating the scattering probability in the Born approximation, we obtain the following equation for the nonequilibrium part of the distribution function $\Delta f_\lambda(\mathbf{k})$:

$$\sum_{\lambda'} \int \frac{d^2k'}{\pi} (1 + \lambda\lambda' \cos[\varphi(\mathbf{k}) - \varphi(\mathbf{k}')]) \delta[\varepsilon_\lambda(\mathbf{k}) - \varepsilon_{\lambda'}(\mathbf{k}')] \times [\Delta f_\lambda(\mathbf{k}) - \Delta f_{\lambda'}(\mathbf{k}')] = \frac{e\mathcal{E}\mathbf{v}_\lambda(\mathbf{k})}{R} \frac{\partial f_0}{\partial \varepsilon}. \quad (11)$$

Here dimensionless quantities are used. Electric field \mathcal{E} is normalized to $E_{s_0}k_{s_0}/e$, group velocity $\mathbf{v}_\lambda = \nabla_{\mathbf{k}}\varepsilon_\lambda(\mathbf{k})$, f_0 is the equilibrium distribution function, and R is the only numerical parameter that appears in this system: $R = V_0^2N/\alpha^2$.

We rewrite the nonequilibrium function in the following form:

$$\Delta f_\lambda(\mathbf{k}) = \frac{e|\mathcal{E}|}{R} \mathcal{F}_\lambda(\mathbf{k}) \frac{\partial f_0}{\partial \varepsilon}. \quad (12)$$

$$\mathcal{F}_{\lambda,r}(\phi, \theta) = \frac{\mathcal{G}_{\lambda,r}(\phi, \theta) + \mathfrak{A}(\theta) + \lambda\mathfrak{B}(\theta) \cos[\varphi_{\lambda,r}(\phi)] + \lambda\mathfrak{C}(\theta) \sin[\varphi_{\lambda,r}(\phi)]}{A + \lambda B \cos[\varphi_{\lambda,r}(\phi)] + \lambda C \sin[\varphi_{\lambda,r}(\phi)]}, \quad (17)$$

where the coefficients A , B , C , \mathfrak{A} , \mathfrak{B} , and \mathfrak{C} are directly determined by (13):

$$A = \sum_{\lambda,r} \int \frac{d\phi}{\pi} M_{\lambda,r}(\phi), \quad (18)$$

$$B = \sum_{\lambda,r} \lambda \int \frac{d\phi}{\pi} M_{\lambda,r}(\phi) \cos[\varphi_{\lambda,r}(\phi)], \quad (19)$$

$$C = \sum_{\lambda,r} \lambda \int \frac{d\phi}{\pi} M_{\lambda,r}(\phi) \sin[\varphi_{\lambda,r}(\phi)]; \quad (20)$$

$$\mathfrak{A}(\theta) = \sum_{\lambda,r} \int \frac{d\phi}{\pi} M_{\lambda,r}(\phi) \mathcal{F}_{\lambda,r}(\phi, \theta), \quad (21)$$

The function $\mathcal{F}_\lambda(\mathbf{k})$ is determined by an equation that in the case of zero temperature can be easily obtained by integrating modulo \mathbf{k} in Eq. (11). In this case, integration is performed over the Fermi contours. Since in some cases the contours have complex shapes, $k(\phi)$ is a multivalued function of ϕ , so we have to divide the contours into parts for which $k(\phi)$ becomes a single-valued function. Each part can be marked with an additional index r , which can vary from 1 to 4 depending on the shape of the Fermi contour. With this in mind, we will add this index to the notations of the functions and integrals defined on the Fermi contours. The $\mathcal{F}_{\lambda,r}(\mathbf{k})$ function defined on the Fermi contour part $k = k_{\lambda,r}(\phi)$ is defined by the following equation:

$$\sum_{\lambda',r'} \int \frac{d\phi'}{\pi} (1 + \lambda\lambda' \cos[\varphi_{\lambda,r}(\phi) - \varphi_{\lambda',r'}(\phi')]) M_{\lambda',r'}(\phi') \times [\mathcal{F}_{\lambda,r}(\phi, \theta) - \mathcal{F}_{\lambda',r'}(\phi', \theta)] = \mathcal{G}_{\lambda,r}(\phi, \theta), \quad (13)$$

where

$$M_{\lambda,r}(\phi) = \left[k \left/ \frac{\partial \varepsilon_\lambda(\mathbf{k})}{\partial k} \right. \right]_{k=k_{\lambda,r}(\phi)}, \quad (14)$$

$$\varphi_{\lambda,r}(\phi) = \varphi(\mathbf{k}) \Big|_{k=k_{\lambda,r}(\phi)}, \quad (15)$$

$$\mathcal{G}_{\lambda,r}(\phi, \theta) = \frac{v_{\lambda,r}(\mathbf{k}) \cos[\xi(\mathbf{k}) - \theta]}{R} \Big|_{k=k_{\lambda,r}(\phi)}. \quad (16)$$

Here $\xi(\mathbf{k})$ is the angle between $\mathbf{v}_{\lambda,r}(\phi)$ and the x axis, and θ is the angle between \mathcal{E} and the x axis. The quantities $M_{\lambda,r}(\phi)$, $\varphi_{\lambda,r}(\phi)$, and $\mathcal{G}_{\lambda,r}(\phi, \theta)$ are determined on the contours corresponding to Fermi energy. They can be easily calculated using Eqs. (4) and (5).

Equation (13) can be solved analytically, since it is a linear Fredholm equation with a degenerate kernel. Representing its kernel as the sum of the products of the functions ϕ and ϕ' (these functions are actually just sines and cosines), we come to the following form of the functions:

$$\mathfrak{B}(\theta) = \sum_{\lambda,r} \lambda \int \frac{d\phi}{\pi} M_{\lambda,r}(\phi) \mathcal{F}_{\lambda,r}(\phi, \theta) \cos[\varphi_{\lambda,r}(\phi)], \quad (22)$$

$$\mathfrak{C}(\theta) = \sum_{\lambda,r} \lambda \int \frac{d\phi}{\pi} M_{\lambda,r}(\phi) \mathcal{F}_{\lambda,r}(\phi, \theta) \sin[\varphi_{\lambda,r}(\phi)]. \quad (23)$$

The coefficients A , B , and C can be directly calculated, since the dispersion law of electrons is known (4). However, the coefficients \mathfrak{A} , \mathfrak{B} , and \mathfrak{C} are determined by integrals containing unknown functions $\mathcal{F}_{\lambda,r}(\phi, \theta)$. To obtain a system of equations that will allow us to find the coefficients \mathfrak{A} , \mathfrak{B} , and \mathfrak{C} , we substitute the expression for them into relation (17). As a result, we get a system of linear algebraic equations for these coefficients. To find the conductivity and spin susceptibility tensors, it is sufficient to carry out the calculation with the orientation of the electric field in the x and y directions ($\theta = 0$

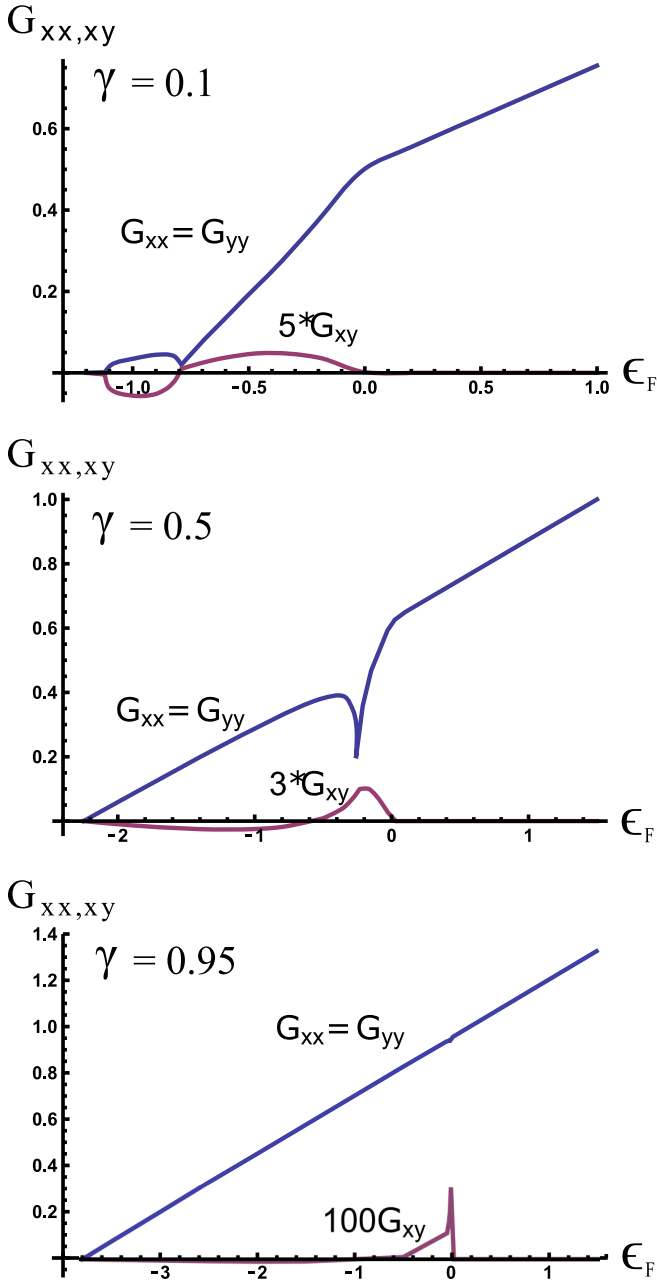


FIG. 4. Dependencies of the components of the conductivity tensor on the Fermi energy for different SOI ratios.

and $\theta = \pi/2$). It should be noted that the determinants of the resulting systems are equal to zero, as well as additional determinants. This indicates the compatibility of the obtained systems and the lack of equations for determining the required coefficients (\mathfrak{A} , \mathfrak{B} , and \mathfrak{C}). Therefore, in each of the obtained systems of equations, one equation is replaced by the electroneutrality equation (this procedure is described in more detail in Ref. [27]).

We make sure that for the orientations of the electric field $\theta = 0$ and $\theta = \pi/2$ the determinant of the obtained systems is not equal to zero and solve them. We find the corresponding coefficients \mathfrak{A} , \mathfrak{B} , and \mathfrak{C} , which we substitute into Eq. (17), thereby we determine the nonequilibrium electron distribution function for these orientations of the electric field.

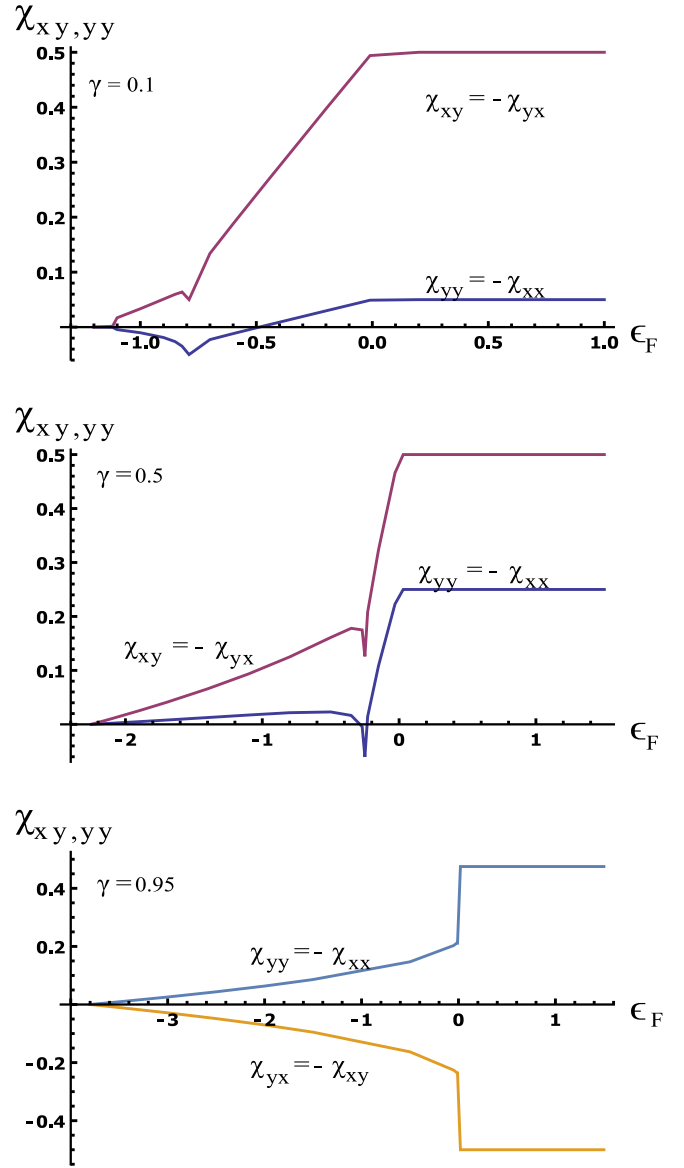


FIG. 5. Components of the Edelstein conductivity tensor as a function of the Fermi energy.

IV. CONDUCTIVITY AND SPIN SUSCEPTIBILITY TENSORS

Using the expression for the distribution function (17), we find the dimensionless components of the conductivity tensor normalized to $e^2/(hR)$:

$$G_{xx} = \sum_{\lambda,r} \int \frac{d\phi}{2\pi} M_{\lambda,r}(\phi) v_{\lambda,r}(\phi) \cos[\xi_{\lambda,r}(\phi)] \mathcal{F}_{\lambda,r}(\phi, 0), \quad (24)$$

$$G_{yx} = \sum_{\lambda,r} \int \frac{d\phi}{2\pi} M_{\lambda,r}(\phi) v_{\lambda,r}(\phi) \sin[\xi_{\lambda,r}(\phi)] \mathcal{F}_{\lambda,r}(\phi, 0). \quad (25)$$

The components of the conductivity tensor G_{xy} and G_{yy} differ from G_{xx} and G_{yx} , respectively, by replacing $\mathcal{F}_{\lambda,r}(\phi, 0)$ with $\mathcal{F}_{\lambda,r}(\phi, \pi/2)$. In Fig. 4 we present the numerical results for

the dependencies of the conductivity tensor components on the Fermi energy for different SOI ratios.

The most interesting is the sharp decrease in the conductivity near the VHS for the SOI ratios in the range defined by inequality (2), as well as the appearance of off-diagonal terms of the conductivity tensor. This corresponds to the appearance of a Hall voltage without a magnetic field due to the anisotropy of the Fermi surface and scattering events. Note also that the anisotropy above the Dirac point completely disappears, as well as near the state of constant spin orientation $\gamma \approx 1$. Note also that the sensitivity of the off-diagonal terms of the conductivity tensor to the Van Hove singularity is higher than that of the diagonal ones (see Fig. 4 for $\gamma = 0.95$).

Since the off-diagonal terms of the conductivity tensor are much smaller than the diagonal terms, the question arises of the reliability of the results obtained. In fact, it is determined by the accuracy of numerical calculations. It is easily estimated by recalculating \mathfrak{A} , \mathfrak{B} , and \mathfrak{C} included in the expression for the nonequilibrium distribution function, as well as calculating the density of states above the Dirac point. As a result, we find that the accuracy of numerical calculations exceeds 10^{-5} . This allows us to consider the obtained dependencies $G_{xy}(\varepsilon_F) = G_{yx}(\varepsilon_F)$ as reliable.

The spin density induced by the electric field is determined by the expression

$$S_i = \frac{\hbar}{2} \sum_{\lambda} \int \frac{d^2k}{4\pi^2} \langle \psi_{\lambda,\mathbf{k}}^\dagger | \sigma_i | \psi_{\lambda,\mathbf{k}} \rangle \Delta f_{\lambda}(\mathbf{k}), \quad (26)$$

where S_i are the spin density components, $i = (x, y, z)$, and σ_i are Pauli matrices. We define the spin susceptibility (it is often called the Edelstein conductivity) as follows:

$$S_i = \sum_j \chi_{ij} \mathcal{E}_j. \quad (27)$$

Using Eqs. (5), (12), and (17), we find for the spin susceptibility

$$\chi_{yx} = \sum_{\lambda,r} \lambda \int \frac{d\phi}{2\pi} M_{\lambda,r}(\phi) \cos[\xi_{\lambda,r}(\phi)] \mathcal{F}_{\lambda,r}(\phi, 0), \quad (28)$$

$$\chi_{xx} = - \sum_{\lambda,r} \lambda \int \frac{d\phi}{2\pi} M_{\lambda,r}(\phi) \sin[\xi_{\lambda,r}(\phi)] \mathcal{F}_{\lambda,r}(\phi, 0). \quad (29)$$

Here the Edelstein conductivity is normalized to $e\hbar/(2\pi\alpha R)$. The components of the spin susceptibility tensor χ_{yy} and χ_{xy} differ from χ_{yx} and χ_{xx} , respectively, by replacing $\mathcal{F}_{\lambda,r}(\phi, 0)$ with $\mathcal{F}_{\lambda,r}(\phi, \pi/2)$. There is no spin polarization along the z axis, $S_z = 0$.

The characteristic features of Edelstein's conductivity as a function of the Fermi energy largely coincide with the features of the conductivity. When the inequality (2) is satisfied, all components of the tensor χ_{ij} have a sharp dip when the Fermi level passes the saddle point. Typical dependencies of this conductivity are shown in Fig. 5. For Fermi energies above the Dirac point, the spin susceptibilities saturate, and the

following relations hold:

$$\chi_{xy} = -\chi_{yx} = 0.5, \quad (30)$$

$$\chi_{yy}/\chi_{xy} = \chi_{xx}/\chi_{yx} = \gamma. \quad (31)$$

V. CONCLUSIONS

The method developed for studying an anisotropic electron transport in a 2DEG in the framework of the Boltzmann kinetic equation [27] is used to calculate the conductivity tensors of a 2DEG with the SOI of Rashba and Dresselhaus types in a wide range of their ratios. This method enables us to accurately find the nonequilibrium distribution function in the case of scattering by impurities with a short-range potential at zero temperature, taking into account the transitions both in one and two different Fermi contours. An important factor determining the conductivity and spin susceptibility tensors is the presence of a Van Hove singularity in the density of states, which arises due to the combined effect of two SOIs. The energy position of the density of states singularities is controlled by the SOI constants ratio. The ratio of the spin susceptibilities, measured at the Fermi energy above the Dirac point, gives the SOIs ratio. The absence of VHS and unconventional dc conductivity indicates a state of persistent spin helix. Note that the depth of the dips near the VHS depends on the "amplitude" of the singularities. Therefore, only if inequality (2) is satisfied, the values of G_{xx} and χ_{xy} tend to zero when Fermi level is near the VHS.

When the second spin subband is filled, the density becomes constant. In addition, interband transitions appear; all this leads to the diagonalization of the conductivity tensor and the disappearance of off-diagonal terms. Earlier this result was obtained in [12]. When the Fermi level crosses the saddle point, the Fermi surface changes significantly [20,22,27], so it is not surprising that this can lead to a change in sign G_{xy} .

Changing the sign of the SOIs ratio $\gamma < 0$ changes the position of saddle points and minima in the \mathbf{k} space and is equivalent to the rotation of the axes in the \mathbf{k} space by $\pi/2$. In turn, this is equivalent to the fact that in all the above expressions we can use $|\gamma|$ instead of γ .

We suppose that the predicted effects can be observed. Difficulties may be associated with the many-particle effects, insufficiently low temperature at which the details may erase, as well as the influence of the fluctuation potential arising with an increase of the concentration of scattering impurities. All these limitations for real observations are well known, and most of them were discussed in detail in [23]. We agree with the statement of [23] that to observe the predicted features, it is enough to use 2D structures with a large SOI (e.g., interfaces between complex oxides). In the same work, there are numerous references to experimental 2D systems that meet the required conditions.

ACKNOWLEDGMENT

The author is grateful to V. A. Sablikov and B. S. Shchamkhalova for useful discussions and criticisms. This work was carried out in the frame of the state task and partially supported by Russian Foundation for Basic Research (Project No. 20-02-00126).

- [1] J. Zutic, J. Fabian, and S. Das Sarma, *Rev. Mod. Phys.* **76**, 323 (2004).
- [2] J. Fabian, A. Matos-Abiague, C. Ertler, P. Stano, and I. Zutic, *Acta Phys. Slovaca* **57**, 565 (2007).
- [3] S. D. Ganichev and L. E. Golub, *Phys. Status Solidi B* **251**, 1801 (2014).
- [4] E. L. Ivchenko and S. D. Ganichev, [arXiv:1710.09223](https://arxiv.org/abs/1710.09223).
- [5] C. R. Ast, J. Henk, A. Ernst, L. Moreschini, M. C. Falub, D. Pacilé, P. Bruno, K. Kern, and M. Grioni, *Phys. Rev. Lett.* **98**, 186807 (2007).
- [6] L. Ye, J. G. Checkelsky, F. Kagawa, and Y. Tokura, *Phys. Rev. B* **91**, 201104 (2015).
- [7] S. V. Eremeev, I. A. Nechaev, Y. M. Koroteev, P. M. Echenique, and E. V. Chulkov, *Phys. Rev. Lett.* **108**, 246802 (2012).
- [8] S. Seri, M. Schultz, and L. Klein, *Phys. Rev. B* **86**, 085118 (2012).
- [9] P. Schwab and R. Raimondi, *Eur. Phys. J. B* **25**, 483 (2002).
- [10] R. Raimondi and P. Schwab, *Phys. Rev. B* **71**, 033311 (2005).
- [11] J. Shliemann and D. Loss, *Phys. Rev. B* **68**, 165311 (2003).
- [12] M. Trushin and J. Shliemann, *Phys. Rev. B* **75**, 155323 (2007).
- [13] O. Chalaev and D. Loss, *Phys. Rev. B* **77**, 115352 (2008).
- [14] K. Vyborny, A. A. Kovalev, J. Sinova, T. Jungwirth, *Phys. Rev. B* **79**, 045427 (2009).
- [15] A. Agarwal, S. Chesi, T. Jungwirth, J. Sinova, G. Vignale, and M. Polini, *Phys. Rev. B* **83**, 115135 (2011).
- [16] E. P. Nakhmedov and O. Alekperov, *Eur. Phys. J. B* **85**, 298 (2012).
- [17] D. Bercioux and P. Lucignano, *Rep. Prog. Phys.* **78**, 106001 (2015).
- [18] C. C. Houghton, E. G. Mishenko, and M. E. Raikh, *Phys. Rev. B* **100**, 165140 (2019).
- [19] R. Winkler, in *Spin-Orbit Coupling Effects in Two-Dimensional Electron and Hole Systems*, edited by J. Kuhn, T. Müller, A. Ruckenstein, F. Steiner, J. Trumper, and P. Wolfle, Springer Tracts in Modern Physics Vol. 191 (Springer, Berlin/Heidelberg, 2003).
- [20] Yu. Ya. Tkach, *JETP Lett.* **104**, 105 (2016).
- [21] L. Van Hove, *Phys. Rev.* **89**, 1189 (1953).
- [22] I. V. Kozlov and Yu. A. Kolisnichenko, *Phys. Rev. B* **99**, 085129 (2019).
- [23] V. Brosco, L. Benfatto, E. Cappelluti, and C. Grimaldi, *Phys. Rev. Lett.* **116**, 166602 (2016).
- [24] A. Johansson, J. Henk, and I. Mertig, *Phys. Rev. B* **93**, 195440 (2016).
- [25] A. Aronov and Y. B. Lyanda-Geller, *JETP Lett.* **50**, 431 (1989).
- [26] V. Edelstain, *Solid State Commun.* **70**, 233 (1990).
- [27] V. A. Sablikov, and Yu. Ya. Tkach, *Phys. Rev. B* **99**, 035436 (2019).
- [28] A. L. Sharpe, E. J. Fox, A. W. Barnard, J. Finney, K. Watanabe, T. Taniguchi, M. A. Kastner, and D. Goldhaber-Gordon, *Science* **365**, 605 (2019).
- [29] M. I. Dyakonov and V. Y. Kachorovski, *Fis. Tecn. Poluprov.* **20**, 178 (1986).
- [30] P. Gambardella and I. Miron, *Philos. Trans. R. Soc., A* **369**, 3175 (2011).

Correction: The support statement in the Acknowledgment section was inappropriately worded and has been fixed.